



Article

# The Bifunctional Effects of Lactoferrin (LFcinB11) in Inhibiting Neural Cell Adhesive Molecule (NCAM) Polysialylation and the Release of Neutrophil Extracellular Traps (NETs)

Bo Lu <sup>1,†</sup>, Si-Ming Liao <sup>1,†</sup>, Shi-Jie Liang <sup>1</sup>, Li-Xin Peng <sup>1</sup>, Jian-Xiu Li <sup>1</sup> , Xue-Hui Liu <sup>2</sup>, Ri-Bo Huang <sup>1,3,\*</sup> and Guo-Ping Zhou <sup>1,3,\*</sup> 

- <sup>1</sup> National Key Laboratory of Non-Food Biomass Energy Technology, National Engineering Research Center for Non-Food Biorefinery, Institute of Biological Science and Technology, Guangxi Academy of Sciences, 98 Daling Road, Nanning 530007, China; lubo@gxas.cn (B.L.); liaosiming@gxas.cn (S.-M.L.); liangshijie@gxas.cn (S.-J.L.); penglixin@gxas.cn (L.-X.P.); jianxiuli@gxas.cn (J.-X.L.)
- <sup>2</sup> Institute of Biophysics, Chinese Academy of Sciences, Beijing 100101, China; xhliu@ibp.ac.cn
- <sup>3</sup> Rocky Mount Life Sciences Institute, Rocky Mount, NC 27804, USA
- \* Correspondence: rbhuang@gxas.cn (R.-B.H.); gpzhou@rmlsi.ac (G.-P.Z.)
- † These authors contributed equally to this work.

**Abstract:** The expression of polysialic acid (polySia) on the neuronal cell adhesion molecule (NCAM) is called NCAM-polysialylation, which is strongly related to the migration and invasion of tumor cells and aggressive clinical status. Thus, it is important to select a proper drug to block tumor cell migration during clinical treatment. In this study, we proposed that lactoferrin (LFcinB11) may be a better candidate for inhibiting NCAM polysialylation when compared with CMP and low-molecular-weight heparin (LMWH), which were determined based on our NMR studies. Furthermore, neutrophil extracellular traps (NETs) represent the most dramatic stage in the cell death process, and the release of NETs is related to the pathogenesis of autoimmune and inflammatory disorders, with proposed involvement in glomerulonephritis, chronic lung disease, sepsis, and vascular disorders. In this study, the molecular mechanisms involved in the inhibition of NET release using LFcinB11 as an inhibitor were also determined. Based on these results, LFcinB11 is proposed as being a bifunctional inhibitor for inhibiting both NCAM polysialylation and the release of NETs.

**Keywords:** migration of tumor cells; neuronal cell adhesion molecule; polysialic acid; polysialyltransferase; polysialyltransferase domain; lactoferrin (LFcinB11); neutrophil extracellular traps (NETs); NMR spectroscopy; chemical shift perturbation



**Citation:** Lu, B.; Liao, S.-M.; Liang, S.-J.; Peng, L.-X.; Li, J.-X.; Liu, X.-H.; Huang, R.-B.; Zhou, G.-P. The Bifunctional Effects of Lactoferrin (LFcinB11) in Inhibiting Neural Cell Adhesive Molecule (NCAM) Polysialylation and the Release of Neutrophil Extracellular Traps (NETs). *Int. J. Mol. Sci.* **2024**, *25*, 4641. <https://doi.org/10.3390/ijms25094641>

Academic Editor: Silvia  
Martina Ferrari

Received: 13 March 2024  
Revised: 17 April 2024  
Accepted: 19 April 2024  
Published: 24 April 2024



**Copyright:** © 2024 by the authors. Licensee MDPI, Basel, Switzerland. This article is an open access article distributed under the terms and conditions of the Creative Commons Attribution (CC BY) license (<https://creativecommons.org/licenses/by/4.0/>).

## 1. Introduction

The expression of polysialic acid (polySia) on neuronal cell adhesion molecule (NCAM) [1–7] is called NCAM polysialylation, which is related to cancer cell migration through interactions between polysialyltransferases (polySTs) and CMP-Sia and polyST and polysialic acid (polySia) [8,9]. More specifically, these interactions actually involve the direct bindings of the Polysialyltransferase Domain (PSTD) to CMP-Sia and PSTD to polySia [10–15]. PSTD is a polybasic motif of 32 amino acids in two polySTs: ST8SiaIV and ST8SiaII [16].

The inhibition of posttranslational modifications (PTMs) is related to a number of diseases, such as cancer and nervous and cardiovascular system diseases. One of the latest advances in research on PTMs is the inhibition of the polysialylation of neuronal cell adhesion molecule (NCAM) [17,18], which is strongly related to the migration and invasion of tumor cells and is associated with aggressive, metastatic disease and poor clinical prognosis in the clinic due to the formation of polysialic acid (poly-Sia) on the surface of NCAM [19–22].

It has been known that NCAM-polySia expression on cancer cells is catalyzed by two polysialyltransferases (polySTs), ST8SiaIV and ST8SiaII; specifically, two polybasic motifs,

Polybasic Region (PBR) and Polysialyltransferase Domain (PSTD) within each polyST, have been found to be critically important for polyST activity based on recent mutation and molecular modeling analyses [16,23]. Thus, the intermolecular interactions of PBR-NCAM, PSTD-polySia, and PSTD-(CMP-sialic acid) have been suggested during NCAM polysialylation and have been tested in more recent NMR studies [14]. Furthermore, a modulation model of NCAM polysialylation and cell migration has been proposed by incorporating the intramolecular interaction of PBR-PSTD into the above intermolecular interaction [14]. This model has been further supported using Chou's wenxiang diagram method [24–28].

Two inhibitors of NCAM polysialylation, low-molecular-weight *heparin* (LMWH) and cytidine monophosphate (CMP), have been proposed in drug research and have shown help in developments related to tumor-targeted polysialyltransferases based on the above modulation model of NCAM polysialylation [16,23].

polyST activity decreased by 93% due to the binding of PSTD-heparin, according to previous in vitro experiments [15]. This finding suggests that heparin is an effective inhibitor of NCAM polysialylation. In recent studies, the binding affinity between the PSTD and three different types of heparin, unfractionated heparin (UFH), heparin tetrasaccharide (DP4), and low-molecular-weight LMWH have been compared using NMR spectroscopy, and it has been further verified that LMWH is the strongest inhibitor among these three types of heparin [21]. However, the use of heparin should be carefully considered, as previous reports have indicated that intracerebral hemorrhages in patients were related to heparin intake [29].

Another inhibitor, cytidine monophosphate (CMP), has also been shown to partially inhibit polysialylation when CMP-Sia and polySia co-exist in solution in recent NMR studies. CMP-Sia may play a role in reducing the extent of accumulation of polySia chains on the PSTD and may be beneficial in inhibiting polysialylation [30]. However, CMP could not inhibit the PSTD–polySia interactions [30].

Different ways to block cancer initiation and progression are of great interest. Many pathways influencing the life of cancer cells may be targeted, including escape from the site of inception or invasion into the metastatic site or death of the cancer cell, such as through necroptosis. One pathway of cell death relevant to some cancers concerns neutrophil extracellular traps (NETs) [31,32]. The activity of NETs may increase during neoplasia, and the rate of cancer growth increases by generating greater amounts of degraded cells. These activations are inhibited by lactoferrin (LF), an iron-binding glycoprotein composed of 49 amino acids. LF has antimicrobial, antiviral, antitumor, and immunological activities [31,32].

It has been described that the LF-derived peptide lactoferricin (LFcin) belongs to the family of antimicrobial peptides [33,34]. LFcin peptide interacts with polySia, and the binding of lactoferrin to polySia is mediated by LFcin, which is included in the N-terminal domain of lactoferrin. The binding between LFcin and polySia was confirmed through the use of native agarose gel electrophoresis [34]. Remarkably, as an antimicrobial peptide, the protective activity of LFcin was not impacted [35,36]. However, previous studies were all conducted at the biochemical, isolated protein level. No works with cultured cell growth models or whole-animal neoplasia models have been undertaken. Before more studies on in vitro work are considered, it is necessary to establish the importance of polySia-LF interaction in vivo in terms of functional effects. The vast majority of reports published to date are either test tube type or use cell cultures. Both are very good in terms of elucidating mechanisms of action but are derivative from a healthcare perspective as they can only be effectively modeled in vivo in intact animals.

In recent studies, a 11-residual peptide (RRWQWRMCKKLG) from the N-terminus [32] of LF was designed LFcinB11, which also has similar antimicrobial activities to those seen in bovine lactoferricin (BLFC) [33,34].

In this study, our aim was to determine whether LFcinB11 can also inhibit NCAM polysialylation. If so, what are the molecular details of this interaction? Previous studies have proposed that the release of neutrophil extracellular traps (NETs) could be inhibited

through the interaction between polySia and LFcIn in in vitro experiments [31–33]. In this study, the molecular details of both LFcIn-PSTD and LFcIn-polySia interactions were explored for the first time using NMR spectra. The results of this study indicate that LFcInB11 may play a bifunctional role in inhibiting the formation of NETs and NCAM polysialylation. These findings may provide a deep insight into drug design for cancer cell inhibition and migration.

## 2. Results

### 2.1. CD Data

As shown in Figure 1, our CD spectra display that the  $\alpha$ -helical content of the PSTD contains 23.0% in the absence of any ligands. The helical contents decreased to 16.4% after adding a mixture of 40  $\mu$ M (CMP-Sia) and 4  $\mu$ M polySia and further decreased to 14.8% after the addition of LFcInB11. These results suggest the helices in the PSTD were unwound due to the addition of the mixture of CMP-Sia and polySia and were further unwound after the addition of LFcInB11. The decreased helical contents in the PSTD indicate its conformational change, verifying that the PSTD not only interacts with the mixture of CMP-Sia and polySia, as shown in previous studies [10–14], but also suggests an interaction between the PSTD and LFcInB11. However, the difference between 16.4% and 14.8% is only 1.6%. This means that the helical structure of the PSTD was basically stable after LFcInB11 was added to the sample. A possible explanation is that there is an interaction between LFcInB11 and polySia. This may be due to the fact that the interaction may decrease the extent of helical unwinding in the PSTD.

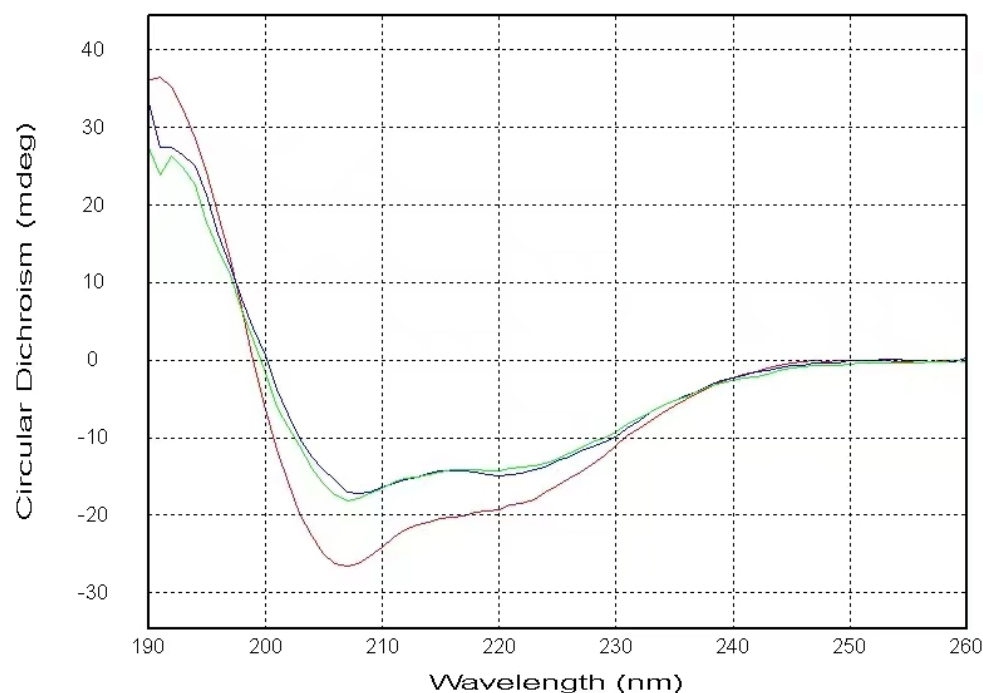


**Figure 1.** The figure shows the CD spectra of the PSTD in the absence (red) and presence of the mixture of CMP-Sia and polySia (green) and the mixture of CMP-Sia, polySia, and LFcInB11 (blue). The helical contents of these three CD spectra of the PSTD are 23%, 16.4%, and 14.8%, respectively.

### 2.2. NMR Results (a)

In order to verify the interaction between the PSTD and LFcInB11, 2D-HSQC experiments involving the mixtures of LFcInB11 with different concentration and the PSTD were carried out. In addition, the PSTD-LFcInB11 interaction was also tested.

### 2.2.1. The Interaction between the PSTD and 20 $\mu$ M LFcInB11

In this study, the overlaid HSQC spectra of the PSTD for the PSTD-(20  $\mu$ M LFcInB11) interaction showed that significant changes in chemical shift could be found in eight residues: K246, K250, V251, R252, T253, S257, V273, and I275 (Table 1 and Figure 2A); most residues are located on the binding region of CMP-Sia (K246-L258) (Table 2), except for two residues: V273 and I275 (Figure 2A). In addition, the CSP values in this range (K246-L258) for the PSTD-20  $\mu$ M LFcInB11 interaction are less than that for the PSTD-(CMP-Sia) interaction (Figure 2). These results indicate that 20  $\mu$ M LFcIn11 could not inhibit the PSTD-(CMP-Sia) interaction. Similarly, the CSPs values in the polySia binding region of the PSTD (A263-N271) are also smaller compared to the PSTD-polySia interaction (Figure 3).

**Table 1.** The table shows the effect of different lactoferrin concentrations (20  $\mu$ M, 40  $\mu$ M, 60  $\mu$ M, and 80  $\mu$ M) on the chemical shift of the residues for the PSTD-LFcInB11 interaction based on the data from Figures 2 and 3.

LFcInB11 Concentration Interacting with the PSTD	Residues in the PSTD That Do Not Change in terms of Chemical Shift	Residues in the PSTD That Changed in relation to Chemical Shift
20 $\mu$ M	17 residues (K248, A254, Y255, L258, R259, V260, I261, H262, A263, V264, R265, Y267, W268, L269, K272, K276, and S279)	8 residues (K246, K250, V251, R252, T253, S257, V273, and I275)
40 $\mu$ M	6 residues (R259, V260, I261, H262, A263, and K272)	19 residues (K246, K248, K250, V251, R252, T253, A254, Y255, S257, L258, V264, R265, Y267, W268, L269, V273, I275, R277, and S279)
60 $\mu$ M	3 residues (R259, V260, and A263)	22 residues
80 $\mu$ M	0 residues	25 residues

**Table 2.** The table shows the binding regions of CMP-Sia and polySia for the different ligands on the PSTD. The maximum CSPs in each binding region are compared with the maximum CSPs for PSTD-(CMP-Sia) and PSTD-polySia interactions, respectively. All CSPs were obtained based on current and previous 2D  $^1$ H- $^{15}$ N HSQC experiments [21,30].

Ligands Binding to the PSTD	The Maximum CSPs in CMP-Sia Binding Region (K246-L258)	The Maximum CSPs in polySia Binding Region (A263-R271)
CMP-Sia	0.063	0.030
polySia	0.031	0.045
Heparin LMWH (80 $\mu$ M)	0.087	0.072
CMP (1 mM)	0.087	0.046
LFcInB11 (20 $\mu$ M)	0.047	0.038
LFcInB11 (40 $\mu$ M)	0.081	0.061
LFcInB11 (60 $\mu$ M)	0.124	0.092
LFcInB11 (80 $\mu$ M)	0.151	0.109

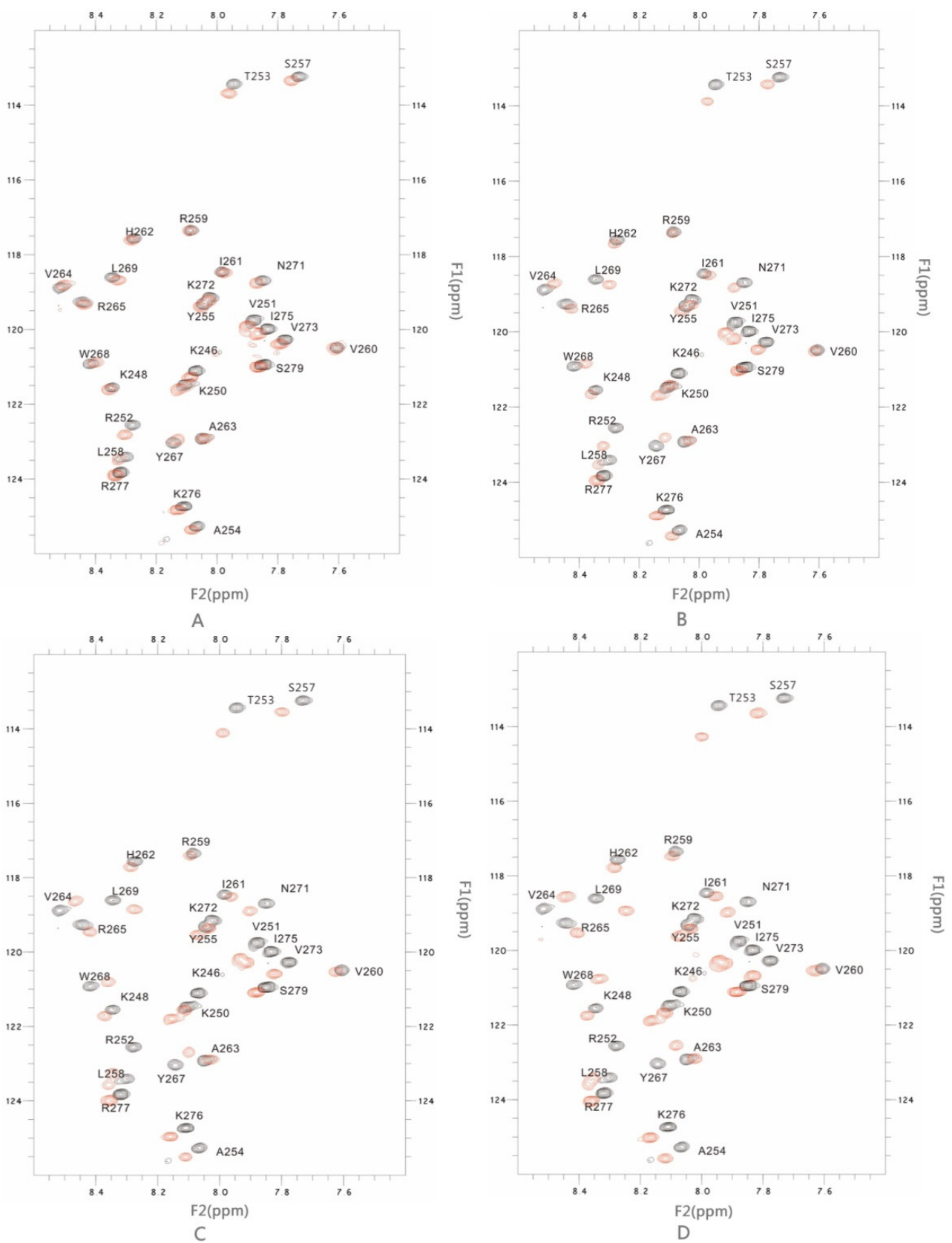
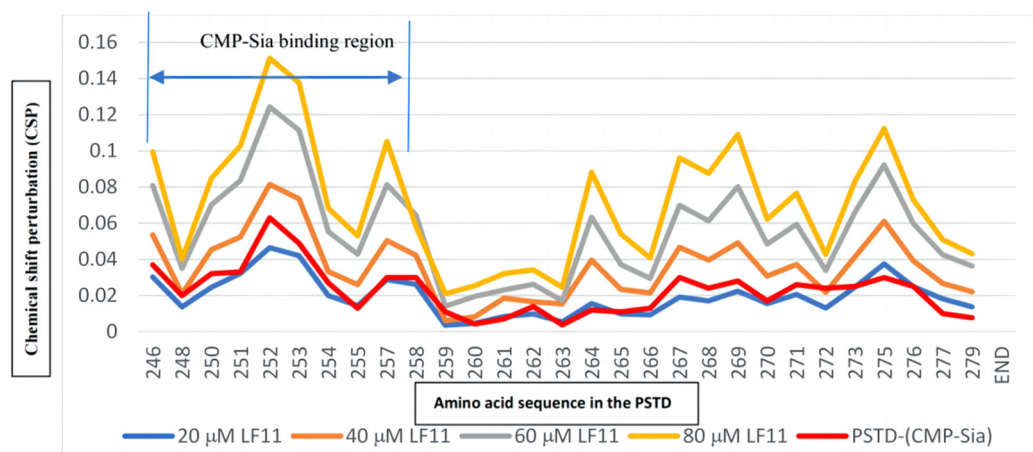
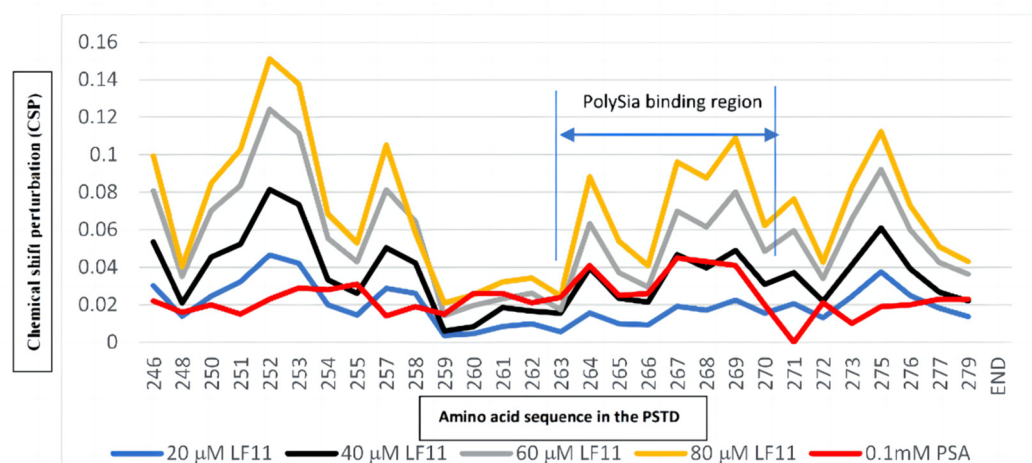


**Figure 2.** The figure shows the overlaid  $^1\text{H}$ - $^{15}\text{N}$  HSQC spectra of the 2 mM PSTD in the absence and presence of 20  $\mu\text{M}$  LFcInB11 (A), 40  $\mu\text{M}$  LFcInB11 (B), 60  $\mu\text{M}$  LFcInB11 (C) and 80  $\mu\text{M}$  LFcInB11 (D), respectively.



A



B

**Figure 3.** The figure shows the chemical shift perturbations (CSPs) of the PSTD when the PSTD interacted with 20  $\mu\text{M}$  LFcinB11 (blue), 40  $\mu\text{M}$  LFcinB11 (orange), 60  $\mu\text{M}$  LFcinB11 (gray), and 1 mM CMP-Sia (red), respectively (A); chemical shift perturbations (CSPs) of the PSTD when the PSTD interacted with 20  $\mu\text{M}$  LFcinB11 (blue), 40  $\mu\text{M}$  LFcinB11 (black), 60  $\mu\text{M}$  LFcinB11 (gray), 80  $\mu\text{M}$  LFcinB11 (orange), and 0.1 mM polySia (red), respectively (B).

### 2.2.2. The Interaction between the PSTD and 40 $\mu\text{M}$ LFcinB11

When the LFcinB11 concentration increased to 40  $\mu\text{M}$ , significant changes in chemical shift were found in 19 residues: K246, K248, K250, V251, R252, T253, A254, Y255, S257, L258, V264, R265, Y267, W268, L269, V273, I275, R277, and S279; there were only six residues (R259, V260, I261, H262, A263, and K272) where no change in chemical shift was observed (Table 1 and Figure 2B). The CSPs for PSTD-40  $\mu\text{M}$  LFcinB11 interaction were larger than that for the PSTD-(CMP-Sia) and PSTD-20  $\mu\text{M}$  LFcinB11 interactions (Figure 3A) in the CMP-Sia binding region, indicating the PSTD-(CMP-Sia) interaction could be inhibited by 40  $\mu\text{M}$  LFcin. In addition, most CSPs for PSTD-40  $\mu\text{M}$  LFcin interaction and the PSTD-polySia interaction are very close in the polySia binding region (Figure 3B). However, the CSPs for the former are larger than that for the latter at residues L269 and N271 (Figure 3B). Thus, this suggests that the PSTD-polySia interaction could be inhibited with a LFcinB11 concentration of more than 40  $\mu\text{M}$ .

### 2.2.3. The Interaction between the PSTD and 60 $\mu$ M LFcInB11

When the LFcInB11 concentration was increased to 60  $\mu$ M, significant changes in chemical shift were found in most residues according to the overlaid HSQC spectra (Figure 2C), and there are only three residues (R259, V260, and A263) where no change in chemical shift was observed (Table 1 and Figure 2C). The CSPs for PSTD-60  $\mu$ M LFcInB11 interaction are larger than that for PSTD-(CMP-Sia) interaction (Figure 3A) in the CMP-Sia binding region, indicating that PSTD-(CMP-Sia) interaction could be inhibited by 60  $\mu$ M LFcInB11. In addition, the CSPs for PSTD-60  $\mu$ M LFcInB11 interaction are also larger than that for PSTD-polySia interactions in the polySia binding region (Figure 3B); thus, this further suggests that PSTD-polySia interactions could be inhibited through the use of 60  $\mu$ M LFcInB11.

### 2.2.4. The Interaction between the PSTD and 80 $\mu$ M LFcInB11

When the LFcInB11 concentration was increased to 80  $\mu$ M, almost all residues of the PSTD changed in relation to their chemical shift (Figure 2D), and the CSP of each residue was larger than that observed for the interactions between the PSTD and 60  $\mu$ M LFcIn. In the CMP-Sia binding region of PSTD-(CMP-Sia) interactions, the maximum CSP is 0.151, which is larger than that observed for the PSTD-60  $\mu$ M LF, and in the polySia binding region, the maximum CSP is 0.109, which is also much larger than that observed for PSTD-60  $\mu$ M LFcInB11 (Table 2). These results indicate that the CSPs in both CMP-Sia and polySia binding regions of the PSTD increased with increasing LF concentrations.

### 2.2.5. The Interactions between LFcInB11 and polySia

In order to determine the interaction between polySia and LFcInB11, the overlaid 2D  $^1\text{H}$ - $^{15}\text{N}$  HSQC spectra were examined using our NMR spectrometer. As shown in Figure 4, no chemical shift was detected except for residue 11 G after polySia and LFcInB11 were mixed. However, the peak intensities of almost all residues were significantly decreased, thus suggesting the interaction between polySia and LFcInB11 through the formation of LFcInB11-polySia aggregates.

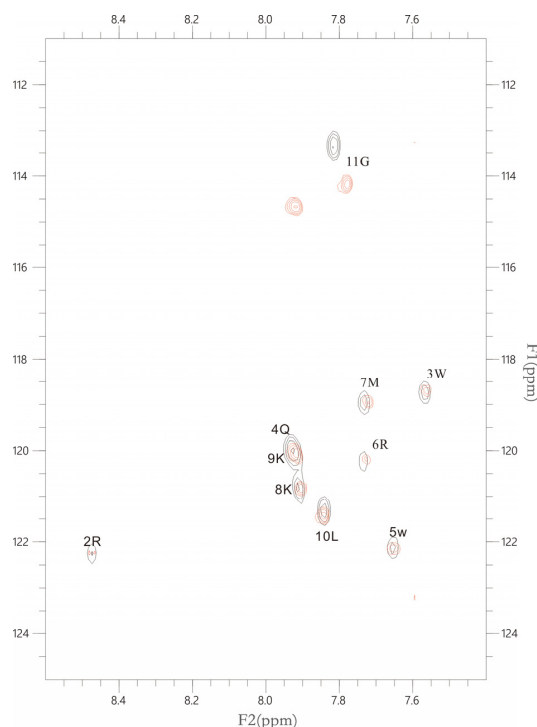


**Figure 4.** The figure shows the overlaid  $^1\text{H}$ - $^{15}\text{N}$  HSQC spectra of 50  $\mu$ M LFcInB11 in the absence (black) and presence of 50  $\mu$ M polySia (red), respectively.

### 3. Discussion

To date, neither 3D X-ray nor NMR structures of polySTs have been reported due to the existence of many hydrophobic residues in polySTs, which are situated in the membrane environment [13,14]. However, a 3D structure of the PSTD peptide in solution, an active site in ST8Sia IV, has been obtained based on our NMR studies [10–14]. Thus, the following hypothesis has been proposed: interactions between the PSTD and ligands, such as CMP-Sia, polySia, or any possible inhibitors, may correspond to interactions between polyST and these ligands. This is an efficient research strategy and methodology for studying biological problems using biophysical and NMR structural biology. The above hypothesis has been successfully tested in recent NMR studies [12,21,30].

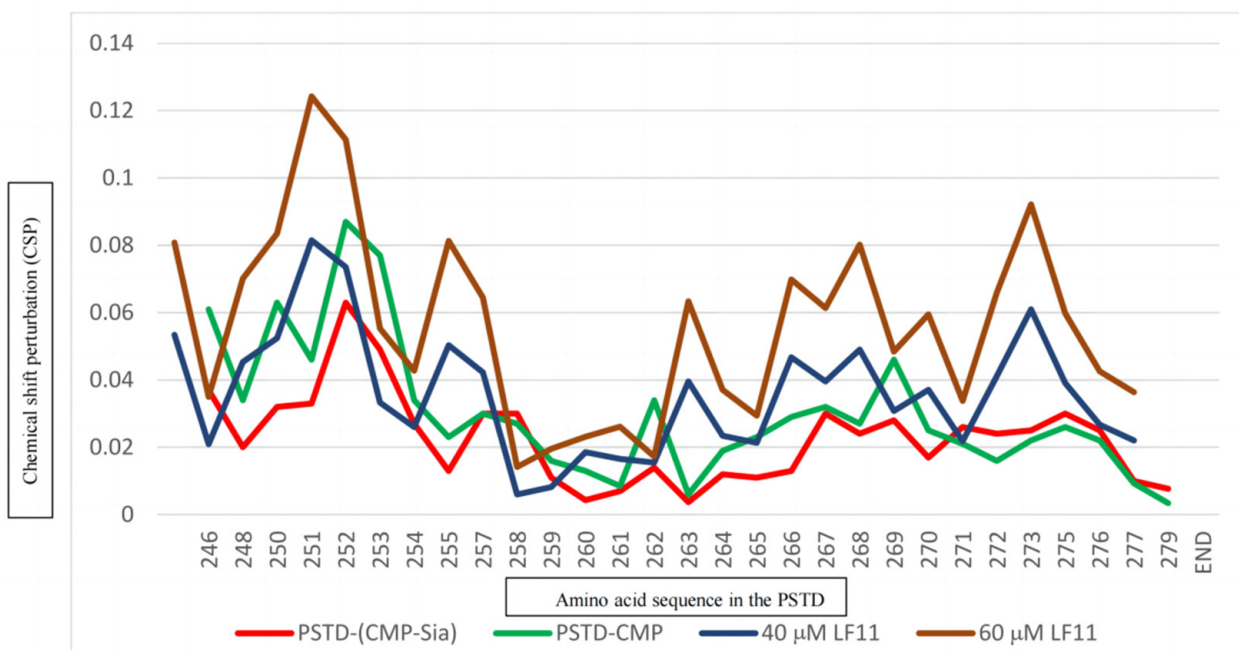
The above CD spectra qualitatively demonstrate the possible interactions between the PSTD and LfcinB11. More details on the interactions between the PSTD and Lfcin11 were provided by our experimental NMR results.

The polysialylation of the trimer of  $\alpha$ -2,8-linked sialic acid (triSia) was inhibited by cytidine monophosphate (CMP) in the presence of ST8SiaII and CMP-Neu5Ac (CMP-Sia) based on *in vitro* experiments [30]. More recent studies have verified that PSTD-(CMP-Sia) could be inhibited by CMP, but PSTD-polySia binding could not be inhibited by CMP, even in a mixture of CMP-Sia, polySia, and the PSTD based on our NMR data [30].

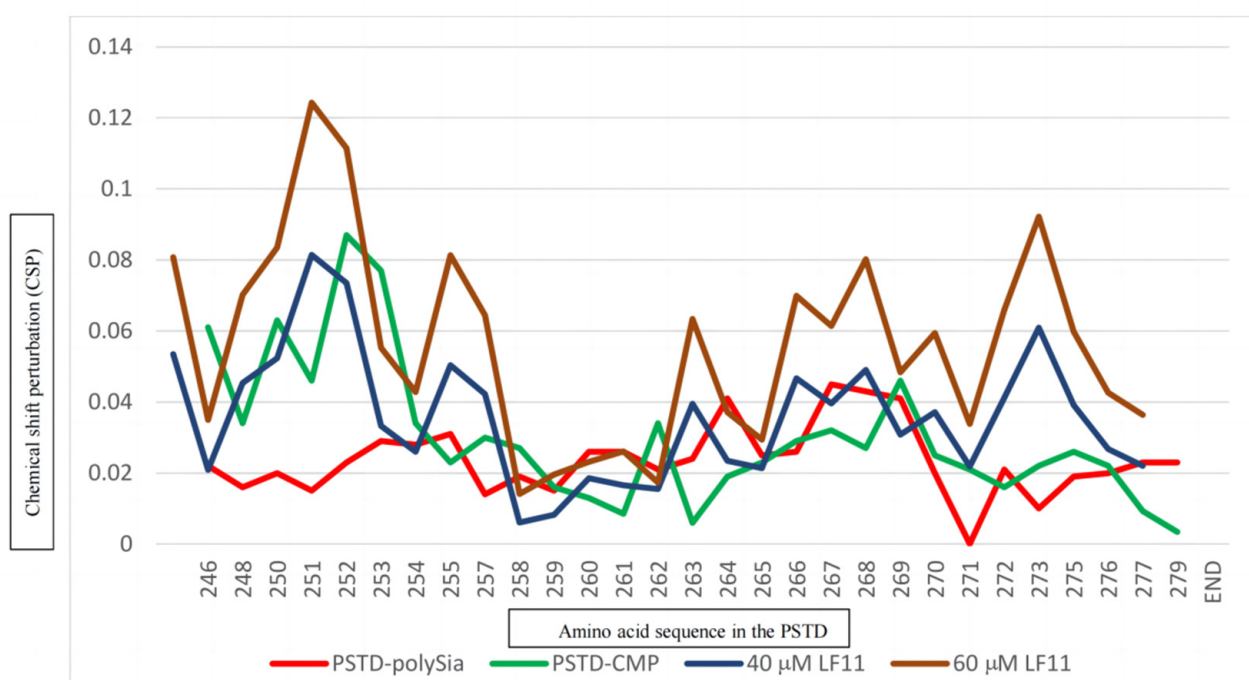
There are two binding regions for CMP-Sia in the PSTD; one is in the residue range of K246-L258, and the other one is in the range of Y267-R277 [30]. The former is also the binding region for CMP, and the latter is covered by the CMP-PSTD binding region (V264-K276) [30]. In this study, the CSP values for the PSTD-LFcinB11 interactions are larger than that for PSTD-CMP and the PSTD-polySia interactions when using a LFcinB11 concentration of at least 40  $\mu$ M (Figure 5). These results indicate that LFcinB11 is more powerful in inhibiting both the PSTD-(CMP-Sia) and PSTD-polySia interactions than CMP.

Previous NMR studies have indicated that LMWH is an effective inhibitor of NCAM polysialylation. Twelve residues, N247, V251, R252, T253, S257, R265, Y267, W268, L269, V273, I275, and K276 in the PSTD were discovered to be the binding sites of LMWH; they were mainly located on the long  $\alpha$ -helix of the PSTD and the short three-residue loop of the C-terminal PSTD [23]. The range of LMWH binding to the PSTD is almost the same as that of the LF (Figure 6). As shown in Figure 6A and Table 2, the CSPs of the PSTD for the PSTD-LMWH (80  $\mu$ M) interaction are larger than that for PSTD-(CMP-Sia) interaction, indicating that PSTD-(CMP-Sia) binding could be inhibited by 80  $\mu$ M LMWH. However, when only taking 40  $\mu$ M LF, both PSTD-(CMP-Sia) interaction and PSTD-polySia interaction could be inhibited (Figure 6B). In addition, as an inhibitor, LFcinB11 may be safer than LMWH due to the fact that intracerebral hemorrhage is related to heparin intake [29].

LFcinB11 can not only interact with the PSTD to inhibit PSTD-(CMP-Sia) and PSTD-polySia interactions but can also directly interact with polySia (Figure 4). This NMR result is consistent with the results obtained when using *in vitro* experiments [32–34] and implies that the major contribution of the interaction between LF and polySia is from the N-terminal residues of LF, particularly in the LFcinB11 domain.

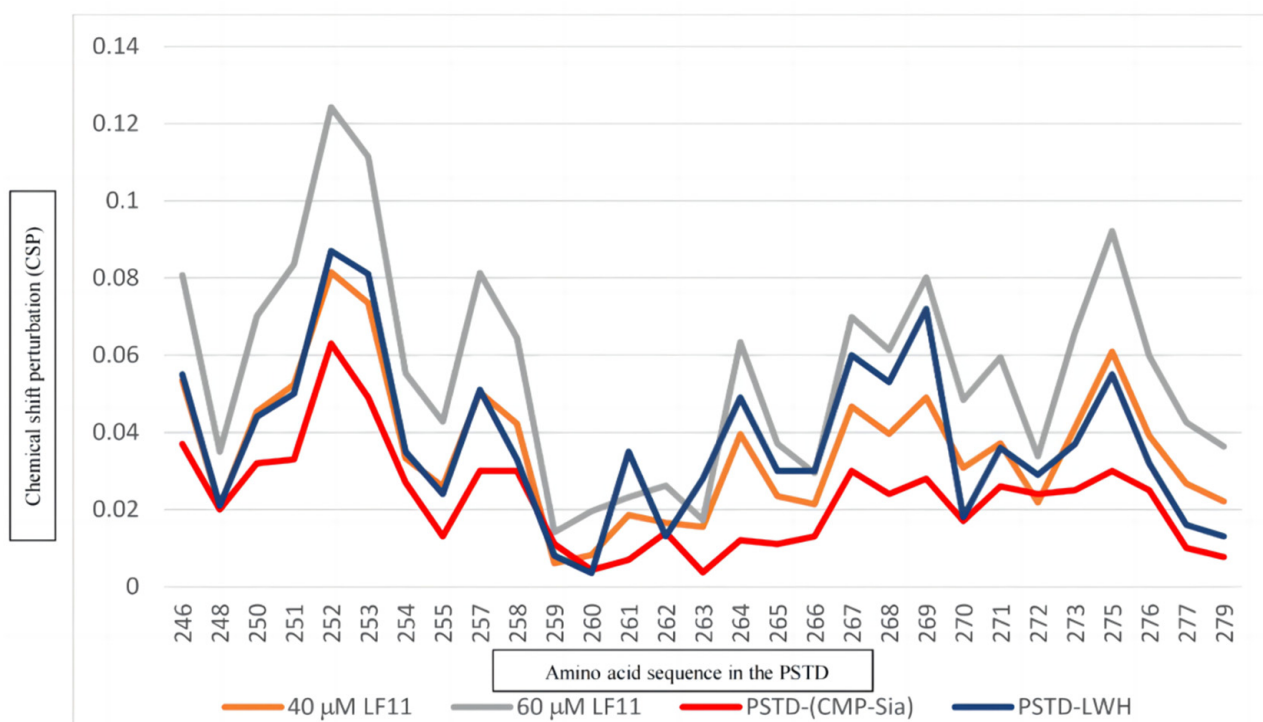


A

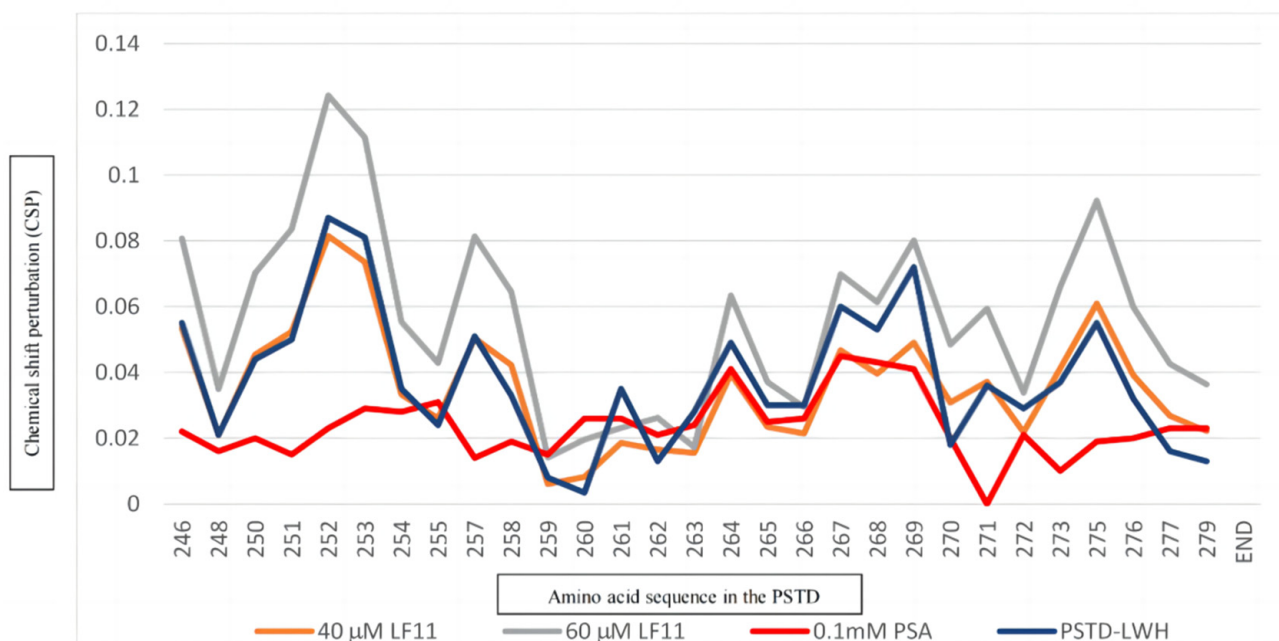


B

**Figure 5.** The figure shows the chemical shift perturbations (CSPs) of the PSTD when interacting with 1 mM CMP-Sia, 80 μM CMP, 40 μM, and 60 μM LFcInB11, respectively (A), and the CSPs of the PSTD when interacting with 0.1 mM PSA, 1 mM CMP, 40 μM, and 60 μM LFcInB11, respectively (B).



A



B

**Figure 6.** The figure shows the chemical shift perturbations (CSPs) of the PSTD when interacting with 1 mM CMP-Sia, 80 μM heparin LMWH, 40 μM, and 60 μM LFcinB11, respectively (A), and the CSPs of the PSTD when interacting with 0.1 mM PSA, 80 μM heparin LWH, and 40 μM and 60 μM LFcinB11, respectively (B).

## 4. Materials and Methods

### 4.1. Material Sources

The PSTD (246K-277R) is a 32 amino acid sequence peptide from the ST8Sia IV molecule, which was derived from human cells [15]. In order to obtain more accurate 3D structural information through the use of NMR spectroscopy, one amino acid (245L) and two amino acids (278P and 279S) from the ST8Sia IV sequence were added to the N- and C- terminals of the PSTD, respectively [12,13]. Thus, a 35 amino acid sequence peptide sample containing the PSTD was synthesized as follows: “245LKNKLVKVRTAYPSLRLLI-HAVRGYWLTKVPIKRPS279”. Herein, the PSTD sequence is underlined. This intact peptide sample was chemically synthesized via automated solid-phase synthesis using the F-MOC-protection strategy and purified through the use of HPLC (GenScript, Nanjing, China). Its molecular weight was determined to be 4117.95 and its purity was established to be 99.36%.

The LFcInB11 peptide was purchased from BACHEM with the following amino sequence RRWQWRMKKLG; it had a relative molecular mass of 1544.8. PolySia was purchased from Santa Cruz Biotechnology.

### 4.2. Circular Dichroism (CD) Spectroscopy

The concentrations of the 35 amino acid-PSTD peptide and LFcInB11 in 20 mM phosphate buffer (pH 6.7) with 25% tetrafluoroethylene (TFE) were 8.0  $\mu\text{M}$  and 400  $\mu\text{M}$ , respectively. The methods used to measure and record the CD spectra were the same as those described in previous articles [23,30].

### 4.3. NMR Sample Preparation

The 35 amino acid peptide containing the PSTD was prepared as described above in a 20 mM phosphate buffer containing 25% TFE. Chemical shifts were referenced with respect to 2-dimethyl-2-silapentane-5-sulfonic acid (DSS), which was used as the internal standard.

For both 1-D and 2-D NMR experiments, the concentration of the PSTD peptide in the absence or presence of LFcInB11 was 2.0 mM. The concentrations of LFcInB11 in the presence of the PSTD were all 20, 40, 60, and 80  $\mu\text{M}$ , respectively. For 2D NMR experiments of polySia-LFcInB11 interaction, the concentrations of polySia and LFcInB11 were all 50  $\mu\text{M}$ .

All of the NMR samples were dissolved in 25% TFE (*v/v*), 10% D<sub>2</sub>O (*v/v*), and 65% (*v/v*) 20 mM phosphate buffer (pH 6.7). Following this, 2-Dimethyl-2-silapentane-5-sulfonic acid (DSS) was added to all samples to serve as a reference standard.

### 4.4. NMR Spectroscopic Methods

NMR spectroscopy is a *powerful* tool for studying biomolecule–protein (DNA) or protein–ligand interactions [36–49]. All of the NMR spectra were recorded at 298 K using an Agilent DD2 800 MHz spectrometer equipped with a cold probe in the NMR laboratory at the Guangxi Academy of Sciences. Water resonance was suppressed using pre-saturation. The NOESY mixing times were set at 300 msec, while the TOCSY experiments were recorded with mixing times of 80 msec [31,50]. All of the chemical shifts were referenced to the internal DSS signal set to 0.00 ppm for protons and indirectly for carbon and nitrogen [21,30]. The data were typically apodized with a shifted sine bell window function and zero-filled to double the data points in F1, prior to being Fourier-transformed. NMRPipe [21,30]. CcpNmr [21] was used to process the data and perform the spectral analysis. Spin system identification and sequential assignment of individual resonances were carried out using a combination of TOCSY and NOESY spectra, as previously described [21,30], and subsequently coupled with an analysis of 1H-15N and <sup>1</sup>H-<sup>13</sup>C HSQC for overlapping resonances. In order to identify and characterize the specificity of PSTD–ligand binding, the chemical shift perturbation (CSP) of each amino acid in the PSTD was calculated using the following formula:

$$\text{CSP} = [(D_{\text{NH}}^2 + (D_{\text{N}}/5)^2)/2]^{1/2} \quad (1)$$

where  $D_N$  and  $D_{NH}$  represent the changes in  $^{15}N$  and  $^1H$  chemical shifts, respectively, upon ligand binding [50–58].

## 5. Conclusions

Our results indicate that LFcIn11 is a more powerful inhibitor than LMWF and CMP and can be safely used. Furthermore, the bifunctional effects of LFcInB11 are proposed, i.e., LFcInB11 can not only inhibit NCAM polysialylation through PSTD-LFcInB11 interaction but can also inhibit the formation of neutrophil extracellular traps (NETs), a network of extracellular strings of DNA that bind to pathogenic microbes [59–70]. Due to the fact that the role of NETs in promoting tumor metastasis formation could be blocked via the addition of LFcIn B11 [71–81], a bifunctional effect of LFcInB11 has been proposed in this study. In future studies, we will further study the molecular mechanism of the interactions between polySia and LFcInB11 to understand how LFcIn blocks tumor metastasis formation related to the formation of NETs.

**Author Contributions:** The manuscript was written with contributions from all authors. Conceptualization, G.-P.Z. and R.-B.H.; Methodology, B.L., J.-X.L. and X.-H.L.; Validation, S.-M.L. and L.-X.P.; Formal Analysis, G.-P.Z.; Investigation, B.L., S.-J.L. and G.-P.Z.; Writing—Original Draft Preparation, G.-P.Z.; Writing—Review and Editing, G.-P.Z.; Supervision, G.-P.Z. and R.-B.H.; Project Administration, S.-M.L.; Funding Acquisition, S.-M.L., B.L. and G.-P.Z. All authors have read and agreed to the published version of the manuscript.

**Funding:** This research was supported by National Natural Science Foundation of China (32060216), Guangxi Science and Technology Base and Talent Project (GuiKe AA20297007), Nanning Scientific Research and Technology Development Project (20223038), Guangxi Major science and technology Innovation base construction project (2022-36-Z06-01), Central Guidance Fund for Local Scientific and Technological Development Project (Guike ZY23055011).

**Institutional Review Board Statement:** Not applicable.

**Informed Consent Statement:** Not applicable.

**Data Availability Statement:** The original contributions presented in the study are included in the article, further inquiries can be directed to the corresponding author/s.

**Acknowledgments:** The authors thank the 800 MHz NMR facility of Guangxi Academy of Sciences for their support in NMR spectra acquirement.

**Conflicts of Interest:** The authors declare no conflicts of interest.

## Abbreviations

polySia	Polysialic acid
Sia	Mono-sialic acid
CMP-Sia	Cytidine monophosphate-sialic acid
NCAMs	Neural cell adhesion molecules
polySTs	Polysialyltransferases (ST8Sia II (STX) and ST8Sia IV (PST))
PSTD	Polysialyltransferase domain
LMWH	Low-molecular-weight heparin
CMP	Cytidine monophosphate
LF	Lactoferrin
CSP	Chemical shift perturbation

## References

1. Lepers, A.H.; Petit, D.; Mollicone, R.; Delannoy, P.; Petit, J.M.; Oriol, R. Evolutionary history of the alpha2,8-sialyltransferase (ST8Sia) gene family: Tandem duplications in early deuterostomes explain most of the diversity found in the vertebrate ST8Sia genes. *Evol. Biol.* **2008**, *8*, 258.
2. Jeanneau, C.; Chazalet, V.; Augé, C.; Soumpasis, D.M.; Harduin-Lepers, A.; Delannoy, P.; Imberty, A.; Breton, C. Structure–function analysis of the human sialyltransferase ST3Gal I: Role of n-glycosylation and a novel conserved sialylmotif. *J. Biol. Chem.* **2004**, *279*, 13461–13468. [[CrossRef](#)] [[PubMed](#)]

3. Sasaki, K.; Kurata, K.; Kojima, N.; Kurosawa, N.; Ohta, S.; Hanai, N.; Tsuji, S.; Nishi, T. Expression cloning of a GM3-specific alpha-2,8-sialyltransferase (GD3 synthase). *J. Biol. Chem.* **1994**, *269*, 15950–15956. [[CrossRef](#)] [[PubMed](#)]
4. Nakayama, J.; Fukuda, M.N.; Hirabayashi, Y.; Kanamori, A.; Sasaki, K.; Nishi, T.; Fukuda, M. Expression cloning of a human GT3 synthase. GD3 AND GT3 are synthesized by a single enzyme. *J. Biol. Chem.* **1996**, *271*, 3684–3691. [[CrossRef](#)] [[PubMed](#)]
5. Johnson, C.P.; Fujimoto, I.; Rutishauser, U.; Leckband, D.E. Direct evidence that neural cell adhesion molecule (NCAM) polysialylation increases intermembrane repulsion and abrogates adhesion. *J. Biol. Chem.* **2005**, *280*, 137–145. [[CrossRef](#)] [[PubMed](#)]
6. Seidenfaden, R.; Krauter, A.; Schertzinger, F.; Gerardy-Schahn, R.; Hildebrandt, H. Polysialic acid directs tumor cell growth by controlling heterophilic neural cell adhesion molecule interactions. *Mol. Cell. Biol.* **2003**, *23*, 5908–5918. [[CrossRef](#)] [[PubMed](#)]
7. Eggers, K.; Werneburg, S.; Schertzinger, A.; Abeln, M.; Schiff, M.; Scharenberg, M.A.; Burkhardt, H.; Mühlenhoff, M.; Hildebrandt, H. Psialic acid controls NCAM signals at cell-cell contacts to regulate focal adhesion independent from FGF receptor activity. *J. Cell Sci.* **2011**, *124 Pt 19*, 3279–3291. [[CrossRef](#)] [[PubMed](#)]
8. Troy, F.A., II. Polysialylation: From bacteria to brains. *Glycobiology* **1992**, *2*, 5–23. [[CrossRef](#)] [[PubMed](#)]
9. Petit, D.; Teppa, E.; Mir, A.M.; Vicogne, D.; Thisse, C.; Thisse, B.; Filloux, C.; Harduin-Lepers, A. Integrative view of  $\alpha$ 2,3-sialyltransferases (ST3Gal) molecular and functional evolution in deuterostomes: Significance of lineage-specific losses. *Mol. Biol. Evol.* **2015**, *32*, 906–927. [[CrossRef](#)] [[PubMed](#)]
10. Zhou, G.-P.; Liao, S.-M.; Chen, D.; Huang, R.-B. The Cooperative Effect between Polybasic Region (PBR) and Polysialyltransferase Domain (PSTD) within Tumor-Target Polysialyltransferase ST8Sia II. *Curr. Top. Med. Chem.* **2020**, *19*, 2831–2841. [[CrossRef](#)] [[PubMed](#)]
11. Liao, S.M.; Lu, B.; Liu, X.H.; Lu, Z.L.; Liang, S.J.; Chen, D.; Troy, F.A., II.; Huang, R.B.; Zhou, G.P. Molecular Interactions of the Polysialyltransferase Domain (PSTD) in ST8Sia IV with CMP-Sialic Acid and Polysialic Acid Required for Polysialylation of the Neural Cell Adhesion Molecule Proteins: An NMR Study. *Int. J. Mol. Sci.* **2020**, *21*, 1590. [[CrossRef](#)] [[PubMed](#)]
12. Liao, S.M.; Liu, X.H.; Peng, L.X.; Lu, B.; Huang, R.B.; Zhou, G.P. Molecular Mechanism of Inhibition of Polysialyltransferase Domain (PSTD) by Heparin. *Curr. Top. Med. Chem.* **2021**, *21*, 1113–1120. [[CrossRef](#)] [[PubMed](#)]
13. Lu, B.; Liu, X.H.; Liao, S.M.; Lu, Z.L.; Chen, D.; Troy, F.A., II.; Huang, R.B.; Zhou, G.P. A Possible Modulation Mechanism of Intramolecular and Intermolecular Interactions for NCAM Polysialylation and Cell Migration. *Curr. Top. Med. Chem.* **2019**, *19*, 2271–2282. [[CrossRef](#)]
14. Zhou, G.P. The Medicinal Chemistry of Structure-based Inhibitor/Drug Design: Current Progress and Future Prospective. *Curr. Top. Med. Chem.* **2021**, *21*, 1097–1098. [[CrossRef](#)] [[PubMed](#)]
15. Nakata, D.; Zhang, L.; Troy, F.A. Molecular basis for polysialylation: A novel polybasic polysialyltransferase domain (PSTD) of 32 amino acids unique to the  $\alpha$ 2,8-polysialyltransferases is essential for polysialylation. *Glycoconj. J.* **2006**, *23*, 423–436. [[CrossRef](#)] [[PubMed](#)]
16. Zhou, G.P.; Chou, K.C. Two Latest Hot Researches in Medicinal Chemistry. *Curr. Top. Med. Chem.* **2020**, *20*, 264–265. [[CrossRef](#)] [[PubMed](#)]
17. Guan, F.; Wang, X.; He, F. Promotion of Cell Migration by Neural Cell Adhesion Molecule (NCAM) Is Enhanced by PSA in a Polysialyltransferase-Specific Manner. *PLoS ONE* **2015**, *10*, e0124237. [[CrossRef](#)] [[PubMed](#)]
18. Elkashef, S.M.; Allison, S.J.; Sadiq, M.; Basheer, H.A.; Morais, G.R.; Loadman, P.M.; Pors, K.; Falconer, R.A. Polysialic acid sustains cancer cell survival and migratory capacity in a hypoxic environment. *Sci. Rep.* **2016**, *6*, 33026. [[CrossRef](#)]
19. Al-Saraireh, Y.M.; Sutherland, M.; Springett, B.R.; Freiburger, F.; Morais, G.R.; Loadman, P.R.; Errington, R.J.; Smith, P.J.; Fukuda, M.; Gerardy-Schahn, R.; et al. Pharmacological inhibition of polysialyltransferase ST8SiaII modulates tumour cell migration. *PLoS ONE* **2013**, *8*, e73366. [[CrossRef](#)]
20. Li, J.; Dai, G.; Cheng, Y.B.; Qi, X.; Geng, M.Y. Polysialylation promotes neural cell adhesion molecule-mediated cell migration in a fibroblast growth factor receptor-dependent manner, but independent of adhesion capability. *Glycobiology* **2011**, *21*, 1010–1018. [[CrossRef](#)]
21. Peng, L.X.; Liu, X.H.; Lu, B.; Liao, S.M.; Zhou, F.; Huang, J.M.; Chen, D.; Troy, F.A., II.; Zhou, G.P.; Huang, R.B. The inhibition of polysialyltransferase st8siaiv through heparin binding to polysialyltransferase domain (PSTD). *Med. Chem.* **2019**, *15*, 486–495. [[CrossRef](#)] [[PubMed](#)]
22. Chou, K.C.; Liu, W.; Maggiora, G.M.; Zhang, C.T. Prediction and Classification of Domain Structural Classes. *Proteins Struct. Funct. Bioinform.* **1998**, *31*, 97–103. [[CrossRef](#)]
23. Chou, K.C.; Maggiora, G.M. Domain Structural Class Prediction. *Protein Eng.* **1998**, *11*, 523–538. [[CrossRef](#)] [[PubMed](#)]
24. Chou, K.-C.; Zhang, C.-T.; Maggiora, G.M. Disposition of amphiphilic helices in heteropolar environments. *Proteins Struct. Funct. Genet.* **1997**, *28*, 99–108. [[CrossRef](#)]
25. Jungck, J.R.; Cebeci, M. Wenxiang 3.0: Evolutionary Visualization of  $\alpha$ ,  $\pi$ , and 3/10 Helices. *Evol. Bioinform.* **2022**, *18*, 11769343221101014. [[CrossRef](#)] [[PubMed](#)]
26. Zhou, G.P.; Huang, R.B. The Graphical Studies of the Major Molecular Interactions for Neural Cell Adhesion Molecule (NCAM) Polysialylation by Incorporating Wenxiang Diagram into NMR Spectroscopy. *Int. J. Mol. Sci.* **2022**, *23*, 15128. [[CrossRef](#)] [[PubMed](#)]
27. Chou, K.-C. The Significant and Profound Impacts of Chou’s “wenxiang” Diagram. *Voice Publ.* **2020**, *6*, 102–103. [[CrossRef](#)]
28. Chou, K.-C.; Lin, W.-Z.; Xiao, X. Wenxiang: A web-server for drawing wenxiang diagrams. *Nat. Sci.* **2011**, *3*, 862–865. [[CrossRef](#)]

29. Babikian, V.L.; Kase, C.S.; Pessin, M.S.; Norrving, B.; Gorelick, P.B. Intracerebral hemorrhage in stroke patients anticoagulated with heparin. *Stroke* **1989**, *20*, 1500–1503. [[CrossRef](#)]
30. Lu, B.; Liao, S.M.; Liu, X.H.; Liang, S.J.; Huang, J.; Lin, M.; Meng, L.; Wang, Q.Y.; Huang, R.B.; Zhou, G.P. The NMR studies of CMP inhibition of polysialylation. *J. Enzyme Inhib. Med. Chem.* **2023**, *38*, 2248411. [[CrossRef](#)]
31. Bellamy, W.; Takase, M.; Yamauchi, K.; Wakabayashi, H.; Kawase, K.; Tomita, M. Identification of the bactericidal domain of lactoferrin. *Biochim. Et Biophys. Acta (BBA)-Protein Struct. Mol. Enzymol.* **1992**, *1121*, 130–136.
32. Gifford, J.L.; Hunter, H.N.; Vogel, H.J. Lactoferricin: A lactoferrin-derived peptide with antimicrobial, antiviral, antitumor and immunological properties. *Cell. Mol. Life Sci.* **2005**, *62*, 2588–2598. [[CrossRef](#)]
33. Kang, J.H.; Lee, M.K.; Kim, K.L.; Hahm, K.S. Structure-biological activity relationships of 11-residue highly basic peptide segment of bovine lactoferrin. *Int. J. Peptide Protein Res.* **1996**, *48*, 357–363. [[CrossRef](#)] [[PubMed](#)]
34. Kühnle, A.; Veelken, R.; Galuska, C.E.; Saftenberger, M.; Verleih, M.; Schuppe, H.C.; Rudlo, S.; Kunz, C.; Galuska, S.P. Polysialic acid interacts with lactoferrin and supports its activity to inhibit the release of neutrophil extracellular traps. *Carbohydr. Polym.* **2019**, *208*, 32–41. [[CrossRef](#)] [[PubMed](#)]
35. Kühnle, A.; Galuska, C.E.; Zlatina, K.; Galuska, S.P. The Bovine Antimicrobial Peptide Lactoferricin Interacts with Polysialic Acid without Loss of Its Antimicrobial Activity against *Escherichia coli*. *Animals* **2020**, *10*, 1. [[CrossRef](#)] [[PubMed](#)]
36. Kühnle, A.; Lutteke, T.; Bornho, K.F.; Galuska, S.P. Polysialic acid modulates the binding of external lactoferrin in neutrophil extracellular traps. *Biology* **2019**, *8*, 20. [[CrossRef](#)]
37. Ortiz, A.I.; Reglero, A.; Rodriguez-Aparicio, L.B.; Luengo, J.M. In vitro synthesis of colominic acid by membrane-bound sialyltransferase of *Escherichia coli* K-235. Kinetic properties of this enzyme and inhibition by CMP and other cytidine nucleotides. *Eur. J. Biochem.* **1989**, *178*, 741–749. [[CrossRef](#)] [[PubMed](#)]
38. Fu, Q.; Piai, A.; Chen, W.; Xia, K.; Chou, J.J. Structure determination protocol for transmembrane domain oligomers. *Nat. Protoc.* **2019**, *14*, 2483–2520. [[CrossRef](#)]
39. Schnell, J.R.; Zhou, G.P.; Zweckstetter, M.; Rigby, A.C.; Chou, J.J. Rapid and accurate structure determination of coiled-coil domains using NMR dipolar couplings: Application to cGMP-dependent protein kinase Ialpha. *Protein Sci.* **2005**, *14*, 2421–2428. [[CrossRef](#)]
40. Sharma, A.K.; Zhou, G.P.; Kupferman, J.; Surks, H.K.; Christensen, E.N.; Chou, J.J.; Mendelsohn, M.E.; Rigby, A.C. Probing the interaction between the coiled coil leucine zipper of cGMP-dependent protein kinase Ialpha and the C terminus of the myosin binding subunit of the myosin light chain phosphatase. *J. Biol. Chem.* **2008**, *283*, 32860–32869. [[CrossRef](#)]
41. Berardi, M.J.; Shih, W.M.; Harrison, S.C.; Chou, J.J. Mitochondrial uncoupling protein 2 structure determined by NMR molecular fragment searching. *Nature* **2011**, *476*, 109–113. [[CrossRef](#)] [[PubMed](#)]
42. OuYang, B.; Xie, S.; Berardi, M.J.; Zhao, X.; Dev, J.; Yu, W.; Sun, B.; Chou, J.J. Unusual architecture of the p7 channel from hepatitis C virus. *Nature* **2013**, *498*, 521–525. [[CrossRef](#)]
43. Oxenoid, K.; Dong, Y.; Cao, C.; Cui, T.; Sancak, Y.; Markhard, A.L.; Grabarek, Z.; Kong, L.; Liu, Z.; Ouyang, B.; et al. Architecture of the mitochondrial calcium uniporter. *Nature* **2016**, *533*, 269–273. [[CrossRef](#)] [[PubMed](#)]
44. Chen, W.; OuYang, B.; Chou, J.J. Critical Effect of the Detergent:Protein Ratio on the Formation of the Hepatitis C Virus p7 Channel. *Biochemistry* **2019**, *58*, 3834–3837. [[CrossRef](#)] [[PubMed](#)]
45. Fu, Q.; Fu, T.M.; Cruz, A.C.; Sengupta, P.; Thomas, S.K.; Wang, S.; Siegel, R.M.; Wu, H.; Chou, J.J. Structural Basis and Functional Role of Intramembrane Trimerization of the Fas/CD95 Death Receptor. *Mol. Cell* **2016**, *61*, 602–613. [[CrossRef](#)] [[PubMed](#)]
46. Joseph, P.R.; Poluri, K.M.; Sepuru, K.M.; Rajarathnam, K. Characterizing protein-glycosaminoglycan interactions using solution NMR spectroscopy. *Methods Mol. Biol.* **2015**, *1229*, 325–333.
47. Bjorndahl, T.C.; Zhou, G.P.; Liu, X.; Perez-Pineiro, R.; Semenchenko, V.; Saleem, F.; Acharya, S.; Bujold, A.; Sobsey, C.A.; Wishart, D.S. Detailed biophysical characterization of the acid-induced PrP(c) to PrP(beta) conversion process. *Biochemistry* **2011**, *50*, 1162–1173. [[CrossRef](#)]
48. Gobl, C.; Madl, T.; Simon, B.; Sattler, M. NMR approaches for structural analysis of multidomain proteins and complexes in solution. *Prog. Nucl. Magn. Reson. Spectrosc.* **2014**, *80*, 26–63. [[CrossRef](#)] [[PubMed](#)]
49. Becker, W.; Bhattacharya, K.C.; Gubensak, N.; Zangger, K. Investigating Protein-Ligand Interactions by Solution Nuclear Magnetic Resonance Spectroscopy. *ChemPhysChem* **2018**, *19*, 895–906. [[CrossRef](#)] [[PubMed](#)]
50. Frueh, D.P. Practical aspects of NMR signal assignment in larger and challenging proteins. *Prog. Nucl. Magn. Reson. Spectrosc.* **2014**, *78*, 47–75. [[CrossRef](#)] [[PubMed](#)]
51. Chalmers, G.R.; Eletsky, A.; Morris, L.C.; Yang, J.Y.; Tian, F.; Woods, R.J.; Moremen, K.W.; Prestegard, J.H. NMR Resonance Assignment Methodology: Characterizing Large Sparsely Labeled Glycoproteins. *J. Mol. Biol.* **2019**, *431*, 2369–2382. [[CrossRef](#)] [[PubMed](#)]
52. Vaynberg, J.; Qin, J. Weak protein-protein interactions as probed by NMR spectroscopy. *Trends Biotechnol.* **2006**, *24*, 22–27. [[CrossRef](#)] [[PubMed](#)]
53. Dominguez, C.; Boelens, R.; Bonvin, A.M.J.J. HADDOCK: A protein-protein docking approach based on biochemical or biophysical information. *J. Am. Chem. Soc.* **2003**, *125*, 1731–1737. [[CrossRef](#)] [[PubMed](#)]
54. Van Zundert, G.C.P.; Rodrigues, J.P.G.L.M.; Trellet, M.; Schmitz, C.; Kastiris, P.L.; Karaca, E.; Melquiond, A.S.J.; van Dijk, M.; de Vries, S.J.; Bonvin, A.M.J.J. The HADDOCK2.2 Web Server: User-Friendly Integrative Modeling of Biomolecular Complexes. *J. Mol. Biol.* **2016**, *428*, 720–725. [[CrossRef](#)] [[PubMed](#)]

55. González-Ruiz, D.; Gohlke, H. Steering Protein-Ligand Docking with Quantitative NMR Chemical Shift Perturbations. *J. Chem. Inf. Model.* **2009**, *49*, 2260–2271. [[CrossRef](#)] [[PubMed](#)]
56. Laveglia, V.; Giachetti, A.; Cerofolini, L.; Haubrich, K.; Fragai, M.; Ciulli, A.; Rosato, A. Automated Determination of Nuclear Magnetic Resonance Chemical Shift Perturbations in Ligand Screening Experiments: The PICASSO Web Server. *J. Chem. Inf. Model.* **2021**, *61*, 5726–5733. [[CrossRef](#)] [[PubMed](#)]
57. Peng, C.; Unger, S.W.; Filipp, F.V.; Sattler, M.; Szalma, S. Automated evaluation of chemical shift perturbation spectra: New approaches to quantitative analysis of receptor-ligand interaction NMR spectra. *J. Biomol. NMR* **2004**, *29*, 491–504. [[CrossRef](#)] [[PubMed](#)]
58. Fino, R.; Byrne, R.; Softley, C.A.; Sattler, M.; Schneider, G.; Popowicz, G.M. Introducing the CSP Analyzer: A novel Machine Learning-based application for automated analysis of two-dimensional NMR spectra in NMR fragment-based screening. *Comput. Struct. Biotechnol. J.* **2020**, *18*, 603–611. [[CrossRef](#)]
59. Williamson, M.P. Using chemical shift perturbation to characterise ligand binding. *Prog. Nucl. Magn. Reson. Spectrosc.* **2013**, *73*, 1–16. [[CrossRef](#)]
60. Williamson, R.A.; Carr, M.D.; Frenkiel, T.A.; Feeney, J.; Freedman, R.B. Mapping the binding site for matrix metalloproteinase on the N-terminal domain of the tissue inhibitor of metalloproteinases-2 by NMR chemical shift perturbation. *Biochemistry* **1997**, *36*, 13882–13889. [[CrossRef](#)]
61. Yadav, R.; Yoo, D.G.; Kahlenberg, J.M.; Bridges, S.L., Jr.; Oni, O.; Huang, H.; Stecenko, A.; Rada, B. Systemic levels of anti-PAD4 autoantibodies correlate with airway obstruction in cystic fibrosis. *J. Cyst. Fibros.* **2019**, *18*, 636–645. [[CrossRef](#)]
62. Brinkmann, V.; Reichard, U.; Goosmann, C.; Fauler, B.; Uhlemann, Y.; Weiss, D.S.; Weinrauch, Y.; Zychlinsky, A. Neutrophil extracellular traps kill bacteria. *Science* **2004**, *303*, 1532–1535. [[CrossRef](#)] [[PubMed](#)]
63. Yoo, D.G.; Winn, M.; Pang, L.; Moskowitz, S.M.; Malech, H.L.; Leto, T.L.; Rada, B. Release of cystic fibrosis airway inflammatory markers from *Pseudomonas aeruginosa*-stimulated human neutrophils involves NADPH oxidase-dependent extracellular DNA trap formation. *J. Immunol.* **2014**, *192*, 4728–4738. [[CrossRef](#)] [[PubMed](#)]
64. Yoo, D.G.; Floyd, M.; Winn, M.; Moskowitz, S.M.; Rada, B. NET formation induced by *Pseudomonas aeruginosa* cystic brosis isolates measured as release of myeloperoxidase-DNA and neutrophil elastase-DNA complexes. *Immunol. Lett.* **2014**, *160*, 186–194. [[CrossRef](#)] [[PubMed](#)]
65. Manzenreiter, R.; Kienberger, F.; Marcos, V.; Schilcher, K.; Krautgartner, W.D.; Obermayer, A.; Huml, M.; Stoiber, W.; Hector, A.; Griese, M.; et al. Ultrastructural characterization of cystic fibrosis sputum using atomic force and scanning electron microscopy. *J. Cyst. Fibros.* **2012**, *11*, 84–92. [[CrossRef](#)]
66. Papayannopoulos, V.; Staab, D.; Zychlinsky, A. Neutrophil elastase enhances sputum solubilization in cystic brosis patients receiving DNase therapy. *PLoS ONE* **2011**, *6*, e28526. [[CrossRef](#)]
67. Li, P.; Li, M.; Lindberg, M.R.; Kennett, M.J.; Xiong, N.; Wang, Y. PAD4 is essential for antibacterial innate immunity mediated by neutrophil extracellular traps. *J. Exp. Med.* **2010**, *207*, 1853–1862. [[CrossRef](#)]
68. Wang, Y.; Li, M.; Stadler, S.; Correll, S.; Li, P.; Wang, D.; Hayama, R.; Leonelli, L.; Han, H.; Grigoryev, S.A.; et al. Histone hypercitullination mediates chromatin decondensation and neutrophil extracellular trap formation. *J. Cell Biol.* **2009**, *184*, 205–213. [[CrossRef](#)]
69. Cheng, H.; Chen, X.; Huan, L. cDNA cloning and sequence analysis of human lactoferrin. *Chin. J. Biotechnol.* **2001**, *17*, 385–387.
70. Le Provost, F.; Nocart, M.; Guerin, G.; Martin, P. Characterization of the goat lactoferrin cDNA: Assignment of the relevant locus to bovine U12 synteny group. *Biochem. Biophys. Res. Commun.* **1994**, *203*, 1324–1332. [[CrossRef](#)]
71. Dwivedi, N.; Radic, M. Citrullination of autoantigens implicates NETosis in the induction of autoimmunity. *Ann. Rheum. Dis.* **2014**, *73*, 483–491. [[CrossRef](#)] [[PubMed](#)]
72. Pang, L.; Hayes, C.P.; Buac, K.; Yoo, D.G.; Rada, B. Pseudogout-associated in ammatory calcium pyrophosphate dihydrate microcrystals induce formation of neutrophil extracellular traps. *J. Immunol.* **2013**, *190*, 6488–6500. [[CrossRef](#)] [[PubMed](#)]
73. Lewis, H.D.; Liddle, J.; Coote, J.E.; Atkinson, S.J.; Barker, M.D.; Bax, B.D.; Bicker, K.L.; Bingham, R.P.; Campbell, M.; Chen, Y.H.; et al. Inhibition of PAD4 activity is sufficient to disrupt mouse and human NET formation. *Nat. Chem. Biol.* **2015**, *11*, 189–191. [[CrossRef](#)] [[PubMed](#)]
74. Cao, X.; Ren, Y.; Lu, Q.; Wang, K.; Wu Wang, Y.; Zhang, Y.; Cui, X.; Yang, Z.; Chen, Z. Lactoferrin: A glycoprotein that plays an active role in human health. *Front. Nutr.* **2023**, *9*, 1018336. [[CrossRef](#)] [[PubMed](#)]
75. Gibbons, J.; Kanwar, R.; Kanwar, J. Lactoferrin and cancer in dierent cancer models. *Front. Biosci.* **2011**, *3*, 1080. [[CrossRef](#)] [[PubMed](#)]
76. Elzoghby, A.O.; Abdelmoneem, M.A.; Hassanin, I.A.; Abd Elwakil, M.M.; Elnaggar, M.A.; Mokhtar, S.; Fang, J.Y.; Elkhodairy, K.A. Lactoferrin, a multi-functional glycoprotein: Active therapeutic, drug nanocarrier & targeting ligand. *Biomaterials* **2020**, *263*, 120355. [[CrossRef](#)]
77. Morgenthau, A.; Pogoutse, A.; Adamiak, P.; Moraes, T.; Schryvers, A. Bacterial receptors for host transferrin and lactoferrin: Molecular mechanisms and role in host-microbe interactions. *Future Microbiol.* **2013**, *8*, 1575–1585. [[CrossRef](#)]
78. Kell, D.; Heyden, E.; Pretorius, E. The biology of lactoferrin, an iron-binding protein that can help defend against viruses and bacteria. *Front. Immunol.* **2020**, *11*, 1221. [[CrossRef](#)] [[PubMed](#)]
79. Lin, T.; Meletharayil, G.; Kapoor, R.; Abbaspourrad, A. Bioactives in bovine milk: Chemistry, technology, and applications. *Nutr. Rev.* **2021**, *79* (Suppl. 2), 48–69. [[CrossRef](#)]

- 
80. Shende, P.; Khanolkar, B. Human breast milk-based nutritherapy: A blueprint for pediatric healthcare. *J. Food Drug Anal.* **2021**, *29*, 203–213. [[CrossRef](#)]
  81. Dierick, M.; Vanrompay, D.; Devriendt, B.; Cox, E. Lactoferrin, a versatile natural antimicrobial glycoprotein that modulates the host's innate immunity. *Biochem. Cell Biol.* **2021**, *99*, 61–65. [[CrossRef](#)] [[PubMed](#)]

**Disclaimer/Publisher's Note:** The statements, opinions and data contained in all publications are solely those of the individual author(s) and contributor(s) and not of MDPI and/or the editor(s). MDPI and/or the editor(s) disclaim responsibility for any injury to people or property resulting from any ideas, methods, instructions or products referred to in the content.